AIP | Review of Scientific Instruments

Note: Near-field imaging of thermal radiation at low temperatures by passive millimeter-wave microscopy

T. Nozokido, M. Ishino, H. Kudo, and J. Bae

Citation: Rev. Sci. Instrum. **84**, 036103 (2013); doi: 10.1063/1.4794911
View online: http://dx.doi.org/10.1063/1.4794911
View Table of Contents: http://rsi.aip.org/resource/1/RSINAK/v84/i3
Published by the American Institute of Physics.

Note: Near-field imaging of thermal radiation at low temperatures by passive millimeter-wave microscopy

T. Nozokido,[1,a)] M. Ishino,[1] H. Kudo,[2] and J. Bae[3]
[1]*Graduate School of Science and Engineering for Research, University of Toyama, 3190 Gofuku, Toyama 930-8555, Japan*
[2]*Department of Computer Science, Graduate School of Systems and Information Engineering, University of Tsukuba, 1-1-1 Tennoudai, Tsukuba 305-8573, Japan*
[3]*Department of Engineering Physics, Electronics, and Mechanics, Nagoya Institute of Technology, Gokiso, Showa-ku, Nagoya 466-8555, Japan*

(Received 29 November 2012; accepted 25 February 2013; published online 6 March 2013)

Imaging of thermal radiation with a spatial resolution below the diffraction limit is demonstrated with a passive millimeter-wave microscope. This technique utilizes a sensitive radiometric receiver in combination with a scanning near-field microscope. Experiments were performed at 50 GHz ($\lambda = 6$ mm) with sample temperatures ranging from room temperature down to 160 K, and the performance was shown to be superior to that achieved with passive imaging systems in the infrared region. The images are affected by non-uniformities in the transmission of thermal radiation from the sample to the receiver via the near-field probe and the reflection of thermal radiation back to the receiver from the probe. The effects of these non-uniformities were successfully removed using a sample image acquired by active measurements using a vector network analyzer. © *2013 American Institute of Physics*. [http://dx.doi.org/10.1063/1.4794911]

Radiometric imaging technologies, which operate at microwave, millimeter wave and submillimeter wave frequencies, have been utilized in various fields, such as radio astronomy, earth remote sensing, security and surveillance, and so on, to form images through the passive detection of naturally occurring incoherent radiation from a scene.[1–3] The spatial resolution achievable with radiometric imaging systems using conventional optics is limited at wavelengths below the operating frequency due to the diffraction effect. To overcome this limitation, we proposed a new type of radiometric imaging technique, passive millimeter-wave microscopy, that permits passive imaging with sub-wavelength spatial resolution by using scanning near-field microscopy and demonstrated the feasibility of this technique at Ka-band (26.5–40 GHz) frequencies for samples at temperatures higher than room temperature using a direct receiver.[4] Imaging of thermal radiation with sub-wavelength spatial resolution using scanning near-field microscopy has also been reported in the infrared region.[5,6] The benefit of using millimeter-wave (radiowave) thermal radiation in this kind of scanning near-field radiometric measurement lies in the promise of carrying out thermal imaging in the low temperature range well below room temperature where passive infrared imaging systems are ineffective. The specification for commercially available passive measuring instruments including thermometers and cameras in the infrared region shows that ∼230 K is the limit of their low temperature operation, whereas in radio astronomy, the 2.7-K cosmic background signature has been successfully observed.[1,7] This limit stems from Planck's law. The brightness of the radiation from a blackbody calculated using Planck's law in the infrared region reduces drastically (deviating from the Rayleigh-Jeans law) as the blackbody temperature decreases below room temperature, whereas in the millimeter-wave region the brightness still obeys the Rayleigh-Jeans law down to ∼1 K. At a blackbody temperature of 50 K, for example, nearly 10^5 times greater brightness is expected in the millimeter-wave region ($\lambda = 6$ mm) compared with that in the infrared region ($\lambda = 10$ μm). We report here imaging results obtained using the passive millimeter-wave microscope system we have developed for this work, with the sample temperature ranging from room temperature down to 160 K.

Figure 1 shows a schematic drawing of our passive millimeter-wave microscope system operating at a millimeter-wave frequency of 50 GHz ($\lambda = 6$ mm). We use a tapered slit-type probe featuring no cutoff as a scanning probe.[8] This type of probe can be operated as a near-field probe over a wide frequency range with high transmission efficiency. The height of the WR-19 rectangular waveguide for U-band (40–60 GHz) frequencies reduces linearly to form a slit aperture at the tip. The height ($h \sim \lambda/60$) and width (w) of the slit aperture are 100 μm and 4.8 mm, respectively. The probe-to-sample separation was adjusted to be 10 μm using a piezoelectric transducer and a laser displacement sensor. Experiments are performed in collection mode. The propagating and evanescent components of the millimeter-wave radiation thermally emitted from the sample are converted via the slit aperture into propagating waves in the probe waveguide, which are then detected by the receiver. The sample to be tested is placed on a copper sample mount, which is temperature-controlled using liquid nitrogen (N_2) as a coolant and an electric heater in combination with a temperature controller operating in on/off or proportional-integral-derivative mode. The temperature of the mount is measured using a thermocouple built into it just beneath the sample. Because the measured temperature can be

a)Author to whom correspondence should be addressed. Electronic mail: nozokido@eng.u-toyama.ac.jp.

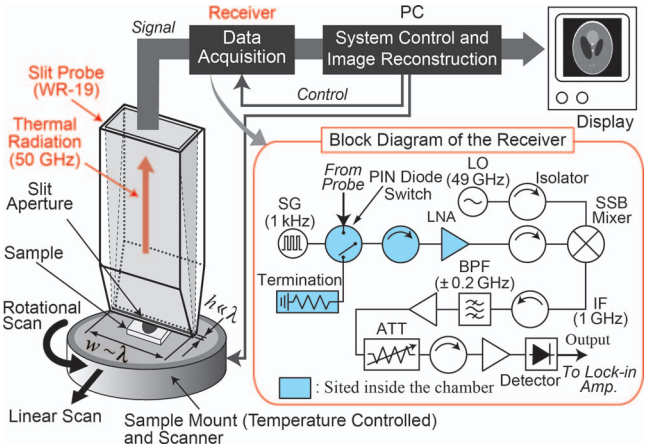

FIG. 1. Experimental setup for passive millimeter-wave microscopy. The inset shows a block diagram of the radiometric receiver.

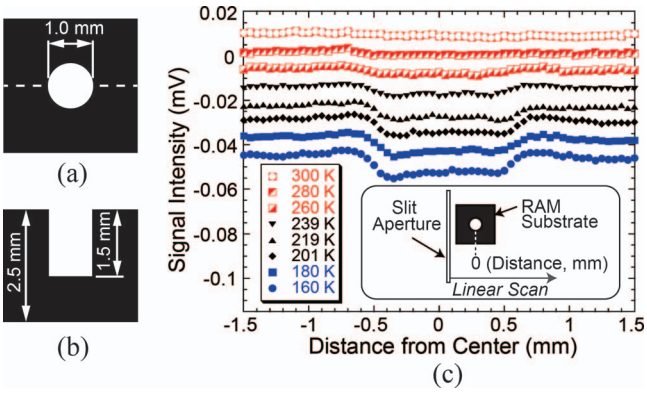

FIG. 2. (a) Schematic diagram of the sample. (b) Cross-sectional drawing of the sample along the dotted line in (a). (c) One-dimensional scans of the sample at various sample temperatures from 300 K to 160 K. The inset in (c) shows the scanning arrangement. The sample is 30 mm in diameter. In (a) and (b), only the area corresponding to the field of view (3 mm × 3 mm) in the imaging experiment (Fig. 3) is depicted.

considered as being almost equal to that of the back surface of the sample in contact with the mount, we refer to this measured temperature as the sample temperature. The measurement system (except part of the receiver) is sited in a chamber in order to prevent the sample surface from becoming frosted. The chamber is filled with dry N_2 gas evaporated from liquid N_2.

The inset in Fig. 1 shows a block diagram of the superheterodyne receiver, which operates in a Dicke-switched mode. The input to the receiver is switched by a PIN diode switch between the probe and a termination with a repetition frequency of 1 kHz. The output port of the switch is connected to a low-noise amplifier, LNA (Gain: 50 dB, NF: 3.2 dB) via an isolator. The remainder of the millimeter-wave and microwave components that comprise the receiver are installed outside the chamber. The output of the LNA is down-converted to an intermediate frequency (IF) signal with a center frequency of 1 GHz by a single-sideband (SSB) mixer. The IF bandwidth is 400 MHz. The IF signal is amplified and then detected using a diode detector. The voltage difference between the outputs from the detector when the probe and the termination are connected is measured by using a lock-in amplifier.

We used a scanning method and an image reconstruction algorithm based on computerized tomography for two-dimensional (2D) image reconstruction in order to facilitate deconvolution of the aperture shape. The sample is scanned linearly at different sample-rotation angles using a scanner with both linear and rotational motor-driven stages. A PC is used to control the scanner, to save raw data collected as projections from the lock-in amplifier, and also to execute image reconstruction by implementing a filtered back-projection (FBP) algorithm.[4,9] A 2D spatial resolution equivalent to the height of the slit aperture can be achieved.[8] Because the measured data are proportional to the line integral of the power of the thermal radiation from the sample transmitted to the probe in the width (w) direction of the aperture, the image reconstructed by the FBP algorithm is a reflection of the 2D power distribution of the thermal radiation in the field of view.[9]

Figures 2(a) and 2(b) show schematics of the sample used in the experiments. The sample was a mirror-polished, 2.5 mm thick, 30 mm diameter substrate made of radar-absorbing material (RAM: CA80, TDK) with a diameter of 1.0 mm, and a 1.5 mm deep hole. The refractive index of the RAM measured at 50 GHz by a transmission measurement technique in free space was $3.20 - j0.51$, from which the emissivity of the sample was calculated to be 0.72. Figure 2(c) shows one-dimensional scans of the sample with the sample temperature varying from 300 K to 160 K. The step size used for the linear scans was 50 μm. The output voltage from the lock-in amplifier is plotted in this figure. A negative output voltage means that the output of the diode detector is smaller when the probe is connected than when the termination is connected. This result confirms that the signal intensity is proportional to the sample temperature, indicating that the probe can detect millimeter-wave thermal radiation emitted from the sample, since the Rayleigh-Jeans law holds true in the millimeter-wave region in this temperature range. Figure 2(c) shows that the difference between the signal intensity when the probe was scanned above the hole and that when the probe was scanned above only the RAM surface increases as the sample temperature becomes lower. By using another thermocouple in contact with the front surface of the sample, we confirmed that the temperature of the front surface of the sample was higher than that at the back surface, and that the difference in these temperatures increases linearly as the sample temperature drops, i.e., a temperature gradient was present through the thickness of the sample. The measured temperature difference was 6 K when the sample temperature was 200 K. Due to this gradient, and because thermal radiation emitted from the bottom of the sample (at a lower temperature) can pass through the aperture of the hole via the inside of the hole, the field strength of the thermal radiation above the hole becomes weaker than that above the RAM surface. This is a possible reason for the observed difference between the signal intensities. The noise temperature of the receiver system was calculated from the dc output voltage of the diode detector with the termination connected (−10.9 mV), the emissivity of the sample (0.72), and the result shown in Fig. 2(c), and found to be 8000 K using the Y-factor method, meaning the

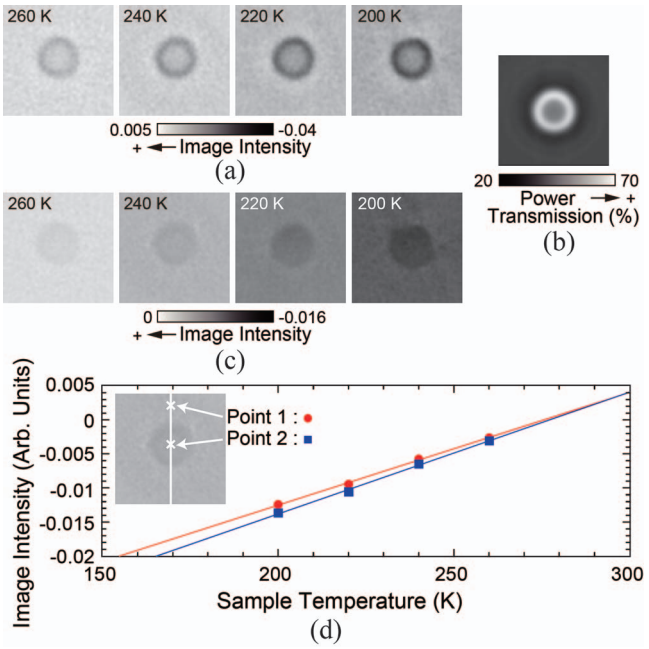

FIG. 3. (a) Reconstructed millimeter-wave images of the sample at various sample temperatures from 260 K to 200 K. (b) Transmission map of the thermal radiation coupled to the probe. (c) Thermal images of the sample calculated from the images in (a) and (b). (d) Image intensity as a function of sample temperature for two distinct points on the reconstructed thermal images of (c) marked with crosses (×) in the inset image. The raw data sets for the images in (a) and (b) were obtained under experimental conditions in which the sampling interval for the linear scan was 50 μm, the number of sampling points was 61, the angle interval for the rotational scan was 6°, and the total number of projections (linear scans) was 31.

temperature resolution of the receiver is 0.8 K with the integration time set to 1 s. These calculated values are not good enough for a sensitive radiometric receiver. This is due to the relatively low power transmission efficiency of the probe used in the experiments (∼30%).

Reconstructed millimeter-wave images of the sample with various sample temperatures from 260 K to 200 K are shown in Fig. 3(a). The time constant of the lock-in amplifier was 1 s. The image size is 3 mm × 3 mm. Although the hole in the sample, whose diameter is less than the wavelength of 50 GHz radiation, can be clearly seen in these images, the images do not accurately reflect the thermal radiation emitted from the sample. This is because the transmission coefficient of the thermal radiation emitted from the sample coupled into the probe waveguide via the slit aperture and the reflection coefficient of the thermal radiation reflected back to the receiver (at room temperature) from the probe are both non-uniform in the field of view. This reflected radiation from the probe is also detected by the receiver. A transmission map showing the distribution of the transmission coefficient is shown in Fig. 3(b). This map changes depending on the sample structure due to near-field interaction between the probe and the sample. The raw data set for the image was acquired by active measurements at 50 GHz using a vector network analyzer (VNA: 8510C, Agilent) at room temperature.[8] The input millimeter-wave power to the probe from the VNA was ∼0.1 mW, which is far greater than that of the thermal radiation. The data set for the reflection coefficient of the probe γ was measured and then the transmission data set $1 - \gamma^2$ was processed into the image using the FBP algorithm. The refection coefficient map is a complementary image of Fig. 3(b). It is possible in our microscope system to correct these transmission and reflection non-uniformities by dividing each of the images in Fig. 3(a) by the image in Fig. 3(b). The resulting thermal images are shown in Fig. 3(c). The intensities of the images in Fig. 3(c) were adjusted to allow direct comparison between Figs. 3(a) and 3(c). Figure 3(d) plots the image intensities at two distinct points in the images shown in Fig. 3(c) as a function of sample temperature. This result shows that the image intensities as well as the signal intensity are proportional to the sample temperature, and that the straight lines fitted to the image intensities for the two points intersect at the laboratory temperature of 300 K, at which the microscope system is in thermal equilibrium. We confirmed from this result that the two lines almost overlap when the intensity for point #1 is plotted against the surface temperature of the RAM.

In conclusion, we have demonstrated near-field imaging of thermal radiation by passive millimeter-wave microscopy, even in the low temperature range where passive infrared imaging systems are ineffective. Since the microscopy format investigated here enables thermal imaging with subwavelength spatial resolution, it is a potential complementary candidate to infrared thermography imaging for microscopic examination in the low temperature range.

This work was supported in part by JSPS KAKENHI Grant No. 22360162.

[1]P. H. Siegel, IEEE Trans. Microwave Theory Tech. **50**, 910 (2002).
[2]L. Yujiri, M. Shoucri, and P. Moffa, IEEE Microw. Mag. **4**, 39 (2003).
[3]R. Appleby and R. N. Anderton, Proc. IEEE **95**, 1683 (2007).
[4]T. Nozokido, M. Noto, and T. Murai, IEEE Microw. Wirel. Compon. Lett. **19**, 638 (2009).
[5]S. Sade, L. Nagli, and A. Katzir, Appl. Phys. Lett. **87**, 101109 (2005).
[6]Y. Kajihara, K. Kosaka, and S. Komiyama, Rev. Sci. Instrum. **81**, 033706 (2010).
[7]J. D. Kraus, *Radio Astronomy*, 2nd ed. (Cygnus-Quasar Books, Durham, 1986), Chap. 8.
[8]T. Nozokido, J. Bae, and K. Mizuno, IEEE Trans. Microwave Theory Tech. **49**, 491 (2001).
[9]A. C. Kak and M. Slaney, *Principles of Computerized Tomographic Imaging* (IEEE, New York, 1988), Chap. 3.